doi: 10.56761/EFRE2022.N3-O-020301

Ti-Mg surface alloys synthesized by Magnetron Sputtering deposition and LEHCEB technique

Chiara Leto[1], Andrea Lucchini Huspek[1], Antonello Vicenzo[1], Silvia Franz[1], Massimiliano Bestetti[1,2,]*

[1]*Department of Chemistry, Materials and Chemical Engineering "Giulio Natta" Politecnico di Milano, Milan, Italy*
[2]*The Weinberg Research Center, Tomsk Polytechnic University, Tomsk, Russia*
[*]*massimiliano.bestetti@polimi.it*

Abstract. Mg and its alloys have attracted a large interest due to a combination of properties such as low density, excellent strength-to-weight ratio, good fatigue and impact strengths, relatively large thermal and electrical conductivities and excellent biocompatibility. This makes Mg alloys very appealing light-weight materials for automotive, consumer electronics and biomedical applications. However, Mg and its alloys have poor corrosion and wear resistance, which limit their applications. Therefore, the possibility of modifying the surface properties of Mg-alloys is nowadays a topic of interest. The aim of the present work is to synthetize and characterize Ti-Mg surface alloys combining PVD deposition of Ti films onto AM60B and AZ91D alloys followed by LEHCEB alloying treatment.
Keywords: Mg-alloys, AM60B, AZ91D, LEHCEB, PVD, Surface treatments.

1. Introduction

Magnesium is one of the most important engineering metals due to its properties, such as low density, high specific strength, good castability and weldability. However, it has poor corrosion resistance, which in general is caused to galvanic coupling, exposure to aggressive environments, and microgalvanic contacts between primary solid solution and second phases [1].

Morini et al. investigated the effects of Low Energy High Current Electron Beam (LEHCEB) treatments on Mg-alloys and, while surface mechanical properties were improved, the corrosion resistance was only slightly increased [2]. Thus, given the results of this previous study, to obtain a beneficial effect in terms of corrosion, surface alloying of AM60B and AZ91D with Ti seemed an effective way to form a stable and enduring protective film. Therefore, that possibility is here investigated with the aim of assessing the performances of a Ti-Mg surface alloy when exposed to an aggressive environment.

The solubility of Ti in Mg at room temperature is negligible, as evidenced by their phase diagram, while the maximum solubility of Mg in solid Ti is 2 at.% at 865 °C [3]. This, in addition with a large difference in melting and boiling points (Ti: T_m 1668 °C, T_b 3287 °C; Mg: T_m 650 °C, T_b 1091 °C), hinders the possibility to create Mg-Ti alloys with conventional casting techniques. To overcome this limitation, it is necessary to work in out-of-equilibrium conditions and different strategies have been tested, such as ion implantation [4], co-sputtering [5] and mechanical alloying [6]. An original procedure was followed in the present work, by depositing a Ti thin film by PVD and then applying a LEHCEB irradiation to obtain a Mg-Ti alloy with a controlled Ti content. Operating parameters for the surface alloying were selected according to COMSOL Multiphysics thermal simulations.

2. Experimental methods

Samples used as substrates were AM60B (Mg 93.2, Al 6.65, Mn 0.15 at.%) and AZ91D (Mg 91.4, Al 8.2, Zn 0.3, Mn 0.1 at.%) magnesium alloys. The samples were 15×32×2 mm^3 (AM60B, q-panel) and 20×15×5 mm^3 (AZ91D, motorcycle wheel rim) in size. A single experimental facility (model RITM-SP, Microsplav "OOO") was employed for both DC Magnetron Sputtering deposition of Ti films and for LEHCEB surface alloying. In this way, the whole process is performed in a single vacuum cycle, avoiding environmental contaminations of any sort. Two values were selected for Ti

thickness, i.e. 500 and 1000 nm. For each thickness two different LEHCEB treatment were performed, the electron accelerating voltage was set at 20 and 25 kV, while pulse number was set at 5 and 10 (pulse duration 2–3 μs and 0.2 Hz repetition frequency). Base pressure in the vacuum chamber was $2 \cdot 10^{-5}$ torr, while working pressure (argon) was $1.8 \cdot 10^{-4}$ and $2.0 \cdot 10^{-3}$ torr for LEHCEB and PVD, respectively. Surface chemical and phase composition were assessed by thin film XRD analysis in grazing angle configuration (Panalytical EMPYREAN PW1830). SEM imaging (Zeiss EVO 50VP) and EDS (Bruker Quantax 200) were performed to investigate surface morphology and elemental composition. GDOES (GDA750 Spectruma Analytik) was employed to obtain compositional depth profiles. Potentiodynamic polarization tests (AMEL Model-2553) at 1 mV/s in aqueous NaCl 3.5 wt% at room temperature, from −500 to 500 mV vs. OCP (open circuit potential) were done to evaluate the corrosion resistance of alloys. A three-electrode set-up, with a KCl saturated Ag/AgCl reference electrode, a platinum mesh as CE and the Mg alloys as WE (0.126 cm^2) was used.

3. Results and discussion

Through COMSOL Multyphysics the melting and evaporation thresholds (i.e. the energy density of a single pulse to induce a phase change in the target material) for the two alloys were calculated. The melting thresholds are 0.73 J/cm^2 for AM60B, 0.74 J/cm^2 for AZ91D and 1.75 J/cm^2 for Ti. The evaporation thresholds are 2.5 J/cm^2 for AM60B, 3.0 J/cm^2 for AZ91D and 3.65 J/cm^2 for Ti. Worth pointing out that thermal simulation results were used to properly choose the operating parameters of the LEHCEB treatment.

XRD spectra in Fig.1 showed the presence of a small intensity peak at 40° which is attributed to the *hcp* Ti. The presence of $Al_{12}Mg_{17}$ intermetallic at 36.1° was also confirmed, this peak was slightly shifted (toward lower angles for AZ91D and toward higher angles for AM60B) and it can be correlated to the cell distortion induced by the presence of Ti.

Table 1. *Hcp* cell parameters *a* and *c* and Ti content for AZ91D and AM60B samples alloyed with Ti

AZ91D					AM60B				
					500 nm				
Sample	**LEHCEB Parameters**	**Ti at. %**	***a* (Å)**	***c* (Å)**	**Sample**	**LEHCEB Parameters**	**Ti at. %**	***a* (Å)**	***c* (Å)**
1	20 kV, 10 p.	10.43	3.1715	5.1561	5	20 kV, 10 p.	8.16	3.1832	5.1594
2	25 kV, 10 p.	9.98	3.1738	5.1564	6	25 kV, 10 p.	8.14	3.1833	5.1702
3	25 kV, 5 p.	10.20	3.1727	5.1615	7	25 kV, 5 p.	8.64	3.1807	5.1724
4	20 kV, 5 p.	10.53	3.1710	5.1534	8	20 kV, 5 p.	8.60	3.1809	5.1646
					1000 nm				
Sample	**LEHCEB parameters**	**Ti at. %**	***a* (Å)**	***c* (Å)**	**Sample**	**LEHCEB Parameters**	**Ti at. %**	***a* (Å)**	***c* (Å)**
9	20 kV, 10 p.	10.60	3.1706	5.1638	13	20 kV, 10 p.	7.81	3.1850	5.1734
10	25 kV, 10 p.	9.29	3.1774	5.1552	14	25 kV, 10 p.	8.09	3.1836	5.1736
11	25 kV, 5 p.	9.76	3.1749	5.1551	15	25 kV, 5 p.	8.59	3.1810	5.1694
12	20 kV, 5 p.	10.79	3.1696	5.1569	16	20 kV, 5 p.	9.05	3.1786	5.1702

Table 1 presents the results of XRD analysis with the calculated *a* and *c hcp* cell parameters, and the Ti at.%. The latter quantity was extrapolated from the data reported by Baliga et al. for the lattice parameters as a function of the atomic Ti content [7], obtaining values ranging from 7 to 10 at.%. This suggested the presence of a Ti-rich outermost surface layer.

Then, corrosion tests were performed and it was possible to assess an increased resistance with respect to the values of the pristine AM60B and AZ91D alloys. Fig.3 shows how the corrosion current density changed for the two alloys, depending on the Ti thickness. There is no apparent trend that could be recognized as an indication of an improvement in the corrosion resistance when depositing

a higher thickness of Ti: in the case of AZ91D samples, passing from 500 to 1000 nm, a decrease in the i_{corr} is found but in the case of AM60B samples the opposite is true. Nor there is a clear indication of which alloy performed better, which may be due the uncertainties of potentiodynamic tests on magnesium alloys. In general, these results show a positive trend with the decrease of the i_{corr} for the samples alloyed with Ti with respect to the pristine ones.

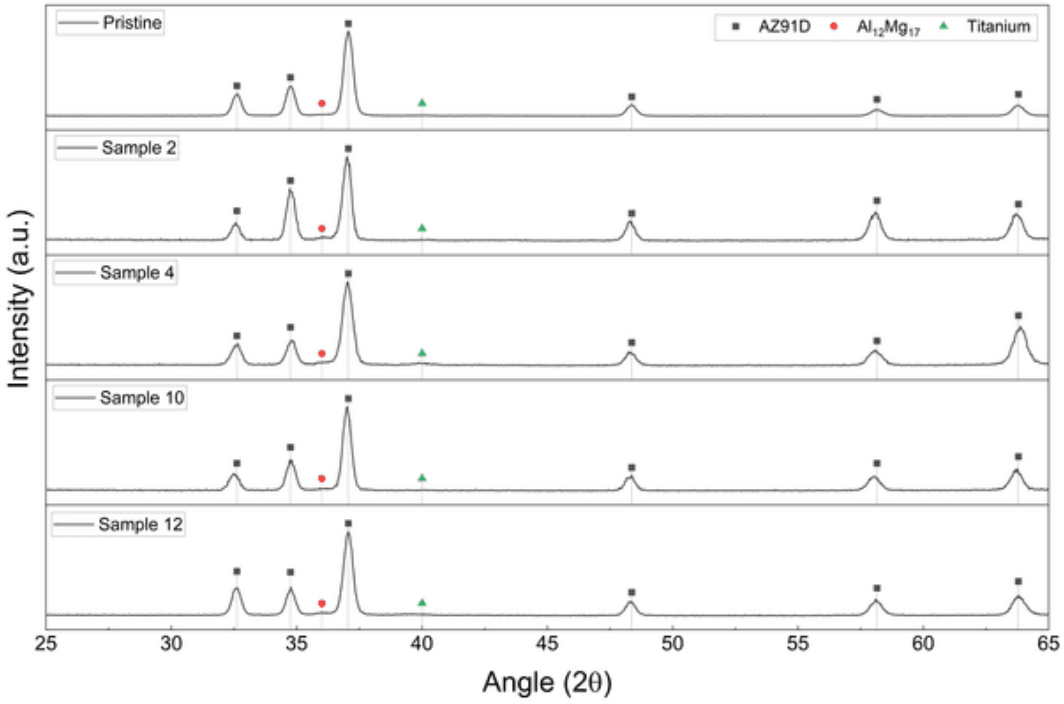

Fig.1: XRD spectra for the AZ91D samples alloyed with 500 nm (sample 1 and 2) and 1000 nm (sample 5 and 6) of Ti compared with pristine AZ91D.

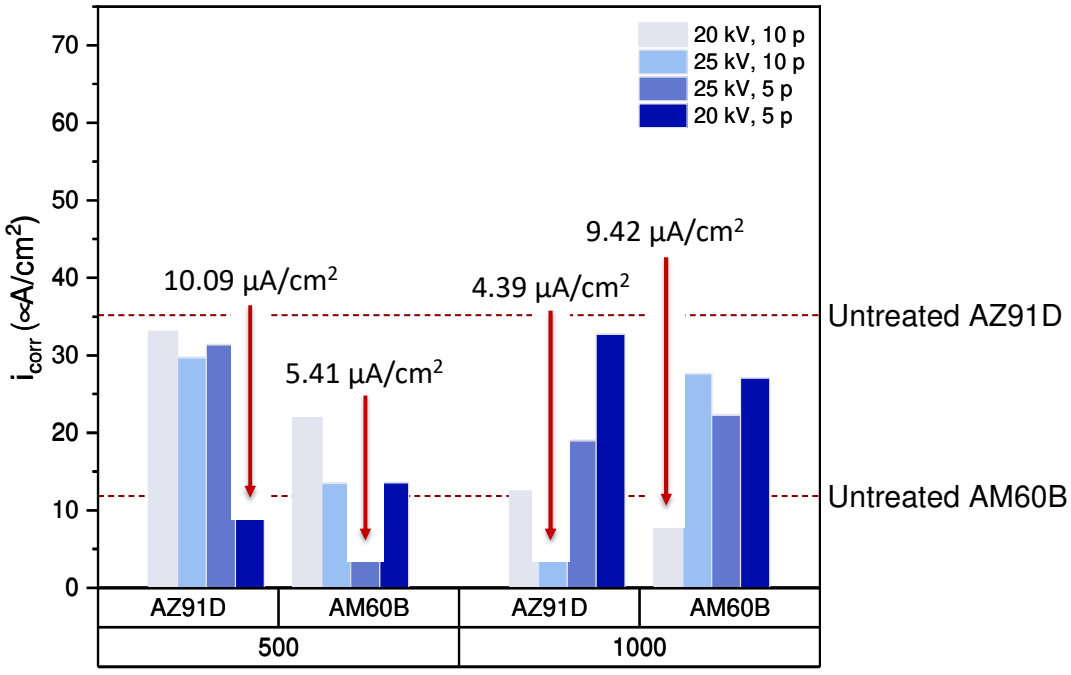

Fig.2. Values of the i_{corr} for the two alloys and 500 and 1000 nm of Ti.

SEM and EDS analyses were performed to assess the microscopic surface morphology and its composition. Six samples were considered: 2, 4, 6, 8, 10 and 12. The choice of analysing samples treated at 25 kV (10 pulses) and at 20 kV (5 pulses) was taken to study the effects of diametral opposite conditions. In Fig.3, it is possible to observe two types of particles: one with size ranging from 1 to 4 μm, the other smaller than 2 μm. According to EDS analyses these two types have different compositions, the larger ones are constituted by segregated Al particles, while the smaller ones are of Ti. It is thus evident that the morphology of surface alloys is quite inhomogeneous.

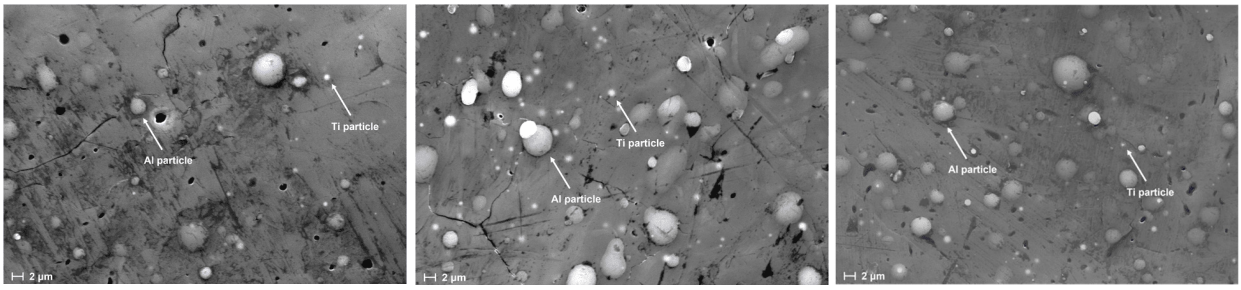

Fig.3. SEM surface morphology of sample 2 (left), 6 (middle) and 10 (right).

In Tables 2 and 3 the i_{corr} and EDS measured Ti at.% are reported, comparing at first different Ti thicknesses and then the two substrates. In Fig.4 are shown the EDS maps for the four AZ91D samples analysed highlighting the surface distribution of Ti.

Table 2. Corrosion current density and mean Ti at.% obtained through EDS analyses for the same alloy at different values of deposited Ti

AZ91D 500 nm			*AZ91D 1000 nm*		
Sample	**Mean Ti at.%**	**i_{corr} (μA/cm^2)**	**Sample**	**Mean Ti at.%**	**i_{corr} (μA/cm^2)**
2	0.09	29.72	10	0.25	4.39
4	0.16	10.09	12	1.13	32.75

Table 3. Corrosion current density and mean Ti at.% obtained through EDS analyses for the same values of deposited Ti, but different alloys

AZ91D 500 nm			*AM60B 500 nm*		
Sample	**Mean Ti at.%**	**i_{corr} (μA/cm^2)**	**Sample**	**Mean Ti at.%**	**i_{corr} (μA/cm^2)**
2	0.09	29.72	6	0.72	13.50
4	0.16	10.09	8	4.86	13.57

By comparing Table 2 with Fig.4, it is possible to notice that where there is a more even distribution of titanium on the surface the corrosion resistance increases. This is true even if the atomic percentage of Ti is low, since surface homogeneity of the alloys plays a fundamental role when considering corrosion resistance. This is particularly evident in the case of AZ91D samples treated at 25 kV with 10 pulses and 20 kV with 5 pulses, since the lower corrosion current density of sample 10, i.e. 4.39 μA/cm^2, corresponds to a more uniform titanium distribution on the surface, even if the mean Ti content is only 0.25 at.%. Differently, the i_{corr} in the second sample is higher (32.75 μA/cm^2), even if the mean Ti content is 1.13 at.% because Ti is unevenly distributed than in the previous case. It becomes obvious that the possibility to achieve a continuous and homogeneous layer of Mg-Ti surface alloy could determine the creation of a protective film, thus inducing an enhancement in the corrosion resistance.

To justify the difference in the Ti at.% found in grazing XRD and EDS analyses, it is necessary to underline that the first has a penetration of few nm, while the latter is in the order of few μm. Thus, there is a Ti enrichment in the outermost surface layer, while underneath Ti is found in smaller quantities being diluted in the alloy.

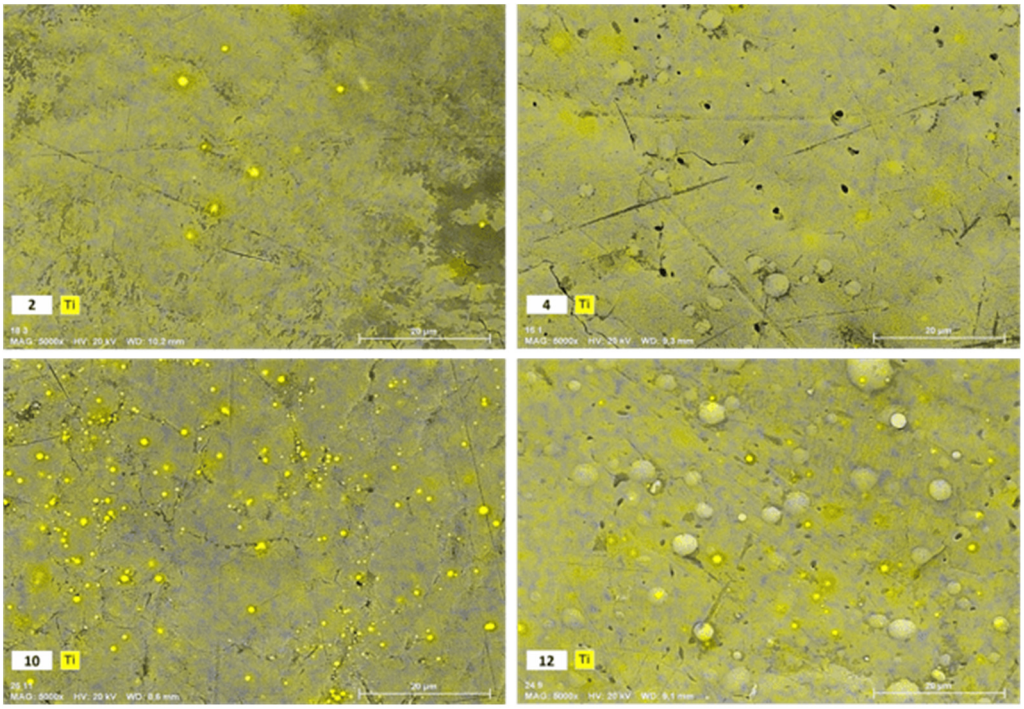

Fig.4. EDS map of Ti (highlighted in yellow) of samples 2, 4, 10, and 12.

Fig.4 displays the GDOES analysis showing that Ti signal has a peak at few hundreds of nanometres in depth and then decreases down to zero within few micrometres. This is a qualitative indication that proves the efficiency of the LEHCEB alloying process in mixing the deposited Ti PVD film with the Mg metallic substrate.

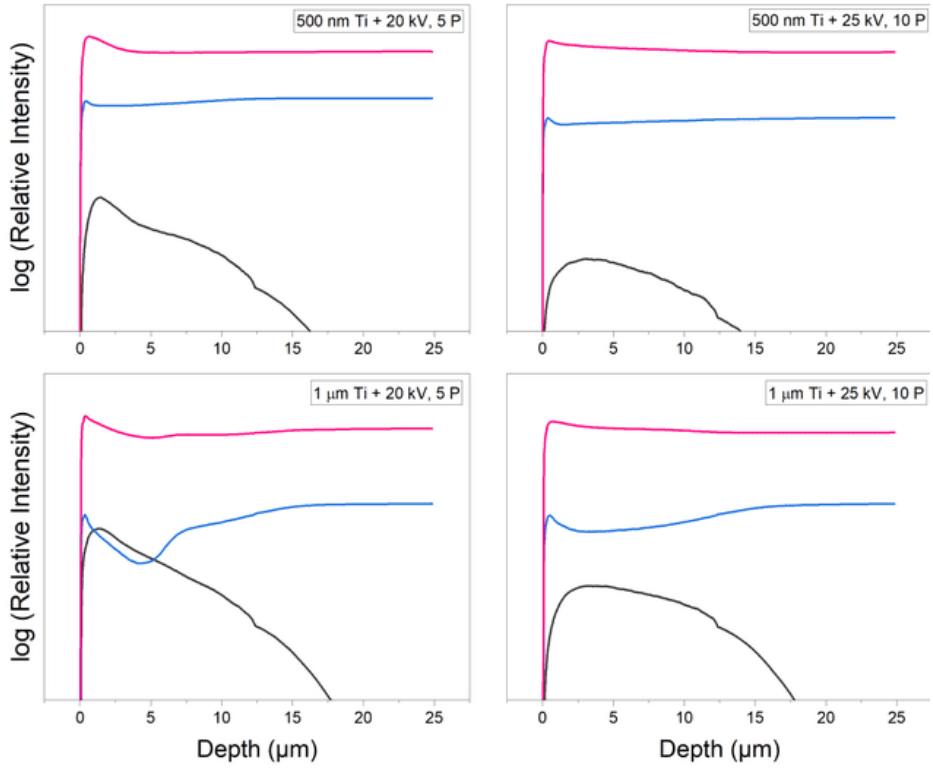

Fig.5. GDOES of samples 2, 4, 10, 12 with Ti signal highlighted in black, Mg in blue and Al in magenta.

4. Conclusion

Mg-Ti surface alloys were successfully synthetized by combining DC Magnetron Sputtering and LEHCEB techniques. Mg-Ti surface alloys were able to increase the resistance to corrosion in most samples. In fact, the i_{corr} changed from 35 μm/cm^2 to a minimum of 9 μm/cm^2 for AZ91D. EDS maps revealed that a more homogeneous distribution contributed to decreasing the i_{corr}. Moreover, the combination of grazing angle XRD and EDS analyses allowed to better understand the structure of the surface alloys. It was observed that the system presents a Ti-rich layer on the surface, while going deeper in the substrate the quantity of Ti decreases, becoming more diluted. Corrosion resistance could be further enhanced with a more homogeneous distribution of Ti obtained by reducing the alloying energy density, or by alternating the deposition of Ti with LEHCEB treatment. A promising new direction for the enhancement of the corrosion resistance could be to alloy the magnesium substrates with rare earth elements [8].

5. References

[1] Candan S., Unal M., Koç E., Turen Y. and Candan E., *J. Alloys Compd.*, **509**, 1958, 2011; doi: 10.1016/j.jallcom.2010.10.100

[2] Morini F., Bestetti M., Franz S., Vicenzo A., Markov A. and Yakovlev E., *Surf. Coat. Technol.*, **420**, 127351, 2021; doi: 10.1016/j.surfcoat.2021.127351

[3] Nayeb-Hashemi A.A., Clark J.B., *Phase diagrams of binary magnesium alloys*. (Ohio: ASM International, 1988).

[4] Liu C., Xin Y., Tian X. and Chu P.K., *Thin Solid Films*, **516**(2–4), 422, 2007; doi: 10.1016/j.tsf.2007.05.048

[5] Xu Z., Song, G.L. and Haddad D., *Magnesium Technology.* (Springer: Cham, 2011); doi: 10.1007/978-3-319-48223-1_112

[6] Wilkes D.M.J., Goodwin P.S., Ward-Close C.M., Bagnall K., and Steeds J., *Mater. Lett.*, **27**(1–2), 47, 1996; doi: 10.1016/0167-577X(95)00265-0

[7] Baliga C.B., Tsakiropoulos P., Dodd S.B. and Gardiner R.W., *Proc. 3rd International Magnesium Conference*, Manchester, 627, 1996.

[8] Azzeddine H., Hanna A., Dakhouche A., Rabahi L., Scharnagl N., Dopita M., Brisset F., Helbert A. and Baudin T., *J. Alloys Compd.*, **829**, 154569, 2020; doi: 10.1016/j.jallcom.2020.154569